Available online at www.sciencedirect.com
ScienceDirect
Journal of Sound and Vibration 305 (2007) 467–480
JOURNAL OF SOUND AND VIBRATION
www.elsevier.com/locate/jsvi

Dynamic stability of rotor-bearing systems subjected to random axial forces

T.H. Young[a,*], T.N. Shiau[b], Z.H. Kuo[a]

[a]*Department of Mechanical Engineering, National Taiwan University of Science and Technology, 43 Section 4, Keelung Road, Taipei 106, Taiwan*
[b]*Department of Mechanical Engineering, National Chung-Cheng University, Taiwan*

Received 1 November 2006; received in revised form 21 March 2007; accepted 15 April 2007
Available online 22 June 2007

Abstract

This paper investigates the lateral vibration of a spinning disk–shaft system supported by a pair of ball bearings and subjected to a pair of random axial forces at both ends. The axial forces are assumed as the sum of a static force and a random process with a zero mean. Due to the random axial forces, the rotor-bearing system may experience parametric random instability under certain situations. In this work, the finite element method is applied to yield a set of discretized system equations first. The set of discretized system equations is partially uncoupled by the modal analysis procedure suitable for gyroscopic systems. The stochastic averaging method is then adopted to obtain Ito's equations for the response amplitudes of the system. Finally the first- and second-moment stability criteria are utilized to determine the stability boundaries of the system. Numerical results show that the rotor-bearing system is always stable in the sense of the first-moment stability, and the effects of the average axial compressive force and the disk mass, which will lower all frequencies of the system, tend to destabilize the second-moment stability of the system.

1. Introduction

Rotor-bearing systems are widely used assemblies for power transmission in various kinds of machinery. However, the vibration and dynamic stability of rotor-bearing systems have been serious problems for mechanical engineers, and the problems become more aggravated due to modern demands for higher rotating speeds and worse working conditions. Therefore, extensive researches on the dynamics of disk-shaft-bearing systems have been conducted in the past few decades [1–8].

In practice, rotor-bearing systems are usually subjected to axial forces due to external reactions. Nelson and McVaugh [9] and Nelson [10] studied the dynamic behavior of rotor-bearing systems using the finite element method. The effects of the rotary inertia, gyroscopic moment and static axial load are considered in their analyses. A computer program was developed by Nevzat Ozguven and Levent Ozkan [11] to calculate the whirl speeds and the unbalance response of multi-bearing rotor systems. The effects of rotary inertia,

*Corresponding author. Tel.: +886 2 27376444; fax: +886 2 27376460.
E-mail address: thyoung@mail.ntust.edu.tw (T.H. Young).

0022-460X/$ - see front matter © 2007 Elsevier Ltd. All rights reserved.
doi:10.1016/j.jsv.2007.04.016

gyroscopic moment, static axial load, internal viscous and hysteretic damping and shear deformation are all included in this program. The internal viscous and hysteretic damping considered is of both non-rotating and rotating types.

In a rotor system, the damping force is usually recognized as non-rotating damping, which depends on the absolute velocity of rotor lateral vibration, and rotating damping, which depends on the relative velocity of the rotor between the lateral vibration and the rotation. The effect of the rotating damping may lead to instability of the rotor system in the supercritical speed range for a freely spinning rotor. However, the effect of the non-rotating damping will raise the instability threshold speed of a freely spinning rotor [8,12].

In real situations, the axial force is often time-dependent. Due to this time-dependent axial force, the rotor system, under certain situations, may experience parametric instability, a different form of instability other than instability induced by the rotating damping. Chen and Ku [13] investigated the dynamic stability of a uniform rotating shaft subjected to periodic axial forces by the finite element method. The rotating shaft is modeled as an Euler–Bernoulli beam or a Timoshenko beam, and Bolotin's method is used to construct the stability boundaries of the system. They found that due to the effect of the gyroscopic moment, unstable regions enlarge as the rotational speed increases. The dynamic behavior of a rotating composite disk–shaft system acted upon by periodic axial forces was reported by Chen and Peng [14]. Liao and Huang [15] analyzed the parametric stability of a spinning pretwisted beam under periodic axial forces by the Rayleigh beam theory. The equation of motion is first discretized by the finite element technique, and the stability boundaries of the system are then derived by the method of multiple scales. Numerical results show that the effects of the spin rate and the mean axial force are unfavorable to the stability of the beam.

Recently, Park and Kim [16] analyzed a four degree-of-freedom spindle system using a new type of slot-restricted gas journal bearings. In order to verify the numerical results, experiments were conducted to find the instability threshold speed of the spindle system. Huang [17] investigated the effect of cracks on the dynamic stability of a high-speed spindle supported by gas bearings with periodically varying speeds. Due to the periodically varying speed, the spindle may experience parametric instability. The dynamic stability of rotating spindles supported by either ball bearings or gas bearings with periodically varying speeds was also reported by Huang and Kung [18].

For random axial forces, Sri Namachchivaya [19] studied the dynamic stability of a rotating shaft under axial excitations. The axial excitations consist of a harmonic term and a stationary stochastic process. It is shown that addition of a non-white noise excitation has a stabilizing effect on the parametric instability of a harmonically excited rotating shaft. Young and Gau [20] extended Liao and Huang's efforts to investigate the parametric random stability of a spinning pretwisted beam subjected to random axial forces. The axial forces are assumed as the sum of a static force and a random process with a zero mean. They found that the effects of the spin rate and the static axial force tend to destabilize the pretwisted beam, and the mean-square stability boundary will not exist any more once the static axial force (or the spin rate) exceeds the buckling load (or the threshold speed) of the pretwisted beam.

The topic of rotor-bearing systems acted upon by random axial forces is interesting for rotor-system engineers and researchers. But, to authors' knowledge, references pertaining to this topic have yet been reported. Therefore, this paper investigates the lateral vibration of a spinning disk–shaft system supported by a pair of ball bearings and subjected to a pair of random axial forces at both ends. First the finite element method is applied to yield a set of discretized system equations. Next the set of discretized system equations is partially uncoupled by the modal analysis procedure suitable for a gyroscopic system. Then the stochastic averaging method is adopted to obtain Ito's equations for the response amplitudes of the system. Finally the first- and second-moment stability criteria are utilized to determine the stability boundaries of the system.

2. Equations of motion

Consider a typical flexible rotor-bearing system that consists of a rigid disk of mass M, a flexible shaft of length L and a pair of ball bearings and is subjected to a pair of axial forces $P(t)$ at both ends, as shown in Fig. 1. In this figure, (X, Y, Z) is an inertial coordinate system with the X-axis being coincident with the centerline of the undeformed rotor. If the axial motion of the rotor can be neglected, the displacements of a

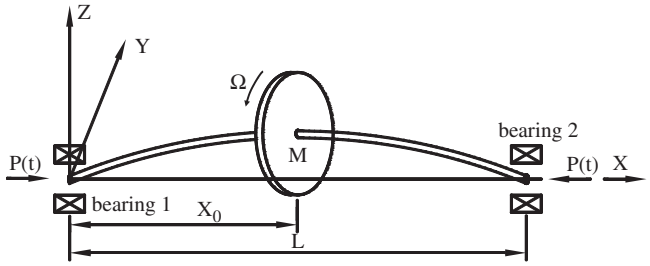

Fig. 1. A rotor-bearing system subjected to random axial forces at both ends.

typical cross-section of the rotor are described by the translations V and W in the Y- and Z-directions and the rotations B and Γ about the Y- and Z-axis, respectively.

In this work, the flexible shaft is assumed as a uniform Timoshenko beam with non-rotating viscous damping coefficient c, and the equations of motion of the shaft are discretized by the finite element method. The ball bearings fit the classical linearized model with eight spring and damping coefficients. In this model, the force at each bearing obeys the governing equations of the form

$$\begin{bmatrix} c_{YY} & c_{YZ} \\ c_{ZY} & c_{ZZ} \end{bmatrix} \begin{Bmatrix} \dot{V} \\ \dot{W} \end{Bmatrix} + \begin{bmatrix} k_{YY} & k_{YZ} \\ k_{ZY} & k_{ZZ} \end{bmatrix} \begin{Bmatrix} V \\ W \end{Bmatrix} = \begin{Bmatrix} f_Y^b \\ f_Z^b \end{Bmatrix}, \tag{1}$$

where c_{ij} and k_{ij} are the elements of the damping and stiffness matrices for the bearing; f_Y^b and f_Z^b are the Y- and Z-components of the bearing force, respectively. The bearing is assumed to be symmetric such that $c_{YZ} = c_{ZY}$ and $k_{YZ} = k_{ZY}$.

The discretized equations of motion of the whole rotor-bearing system can be obtained by assembling the equations for each component, that is, the equations for the rigid disk, flexible shaft and discrete bearings, as [5,9]

$$\mathbf{M}\ddot{\mathbf{q}} + (\alpha\mathbf{C} - \Omega\mathbf{G})\dot{\mathbf{q}} + (\mathbf{K}_e - \mathbf{P}\mathbf{K}_g)\mathbf{q} = \mathbf{Q}, \tag{2}$$

where $\mathbf{M}$ and $\mathbf{G}$ are the mass and gyroscopic matrices of the whole system, respectively. $\mathbf{C}$ is the damping matrix due to the shaft and bearings, and α is a damping factor. $\mathbf{K}_e$ and $\mathbf{K}_g$ are the elastic and geometric stiffness matrices, respectively. $\mathbf{Q}$ is the force vector due to the mass unbalance. $\mathbf{q}$ is the generalized displacement vector, and an overdot denotes a differentiation with respect to time t. All the matrices are symmetric except the gyroscopic matrix $\mathbf{G}$ that is skew symmetric. Usually, the mass unbalance is a major excitation source for flexural vibration of a rotor system. It will induce the so-called "the first-order resonance" of a rotor system. However, we are interesting primarily in the dynamic stability of the rotor system due to the action of the random axial force here, and the stability problem is governed by the corresponding homogeneous equation. Therefore, the non-homogeneous forcing term due to the mass unbalance is neglected in the subsequent analysis.

Eq. (2) is a set of the second-order ordinary differential equations with variable coefficients. To improve the solvability of Eq. (2), a modal analysis procedure suitable for gyroscopic systems [21] is applied to uncouple the undamped, autonomous terms in the system equations. In this work, the axial force is assumed as the sum of a static force P_0 and a weakly stationary random process with a zero mean $P_1(t)$. Therefore, the homogeneous counterpart of Eq. (2) can be rewritten into a set of the first-order differential equations of the form

$$\begin{bmatrix} \mathbf{M} & \mathbf{0} \\ \mathbf{0} & \mathbf{K} \end{bmatrix} \dot{\mathbf{a}} + \begin{bmatrix} -\Omega\mathbf{G} & \mathbf{K} \\ -\mathbf{K} & \mathbf{0} \end{bmatrix} \mathbf{a} = -\alpha \begin{bmatrix} \mathbf{C} & \mathbf{0} \\ \mathbf{0} & \mathbf{0} \end{bmatrix} \mathbf{a} + P_1(t) \begin{bmatrix} \mathbf{0} & \mathbf{K}_g \\ \mathbf{0} & \mathbf{0} \end{bmatrix} \mathbf{a}, \tag{3}$$

where $\mathbf{K} = \mathbf{K}_e + \mathrm{P}_0\mathbf{K}_g$, and $\mathbf{a} = \begin{Bmatrix} \dot{\mathbf{q}} \\ \mathbf{q} \end{Bmatrix}$. Consider the corresponding undamped, autonomous system of Eq. (3), that is the system defined by the left-hand side of the equation. The eigenvalues of the undamped, autonomous system appear in pure imaginary conjugate pairs, i.e., $\lambda_n = \pm \mathrm{i}\omega_n$, $n = 1, 2, \ldots, N$, where ω_n are the frequencies of the rotor-bearing system under the action of the static axial force P_0, and N is the total degrees of freedom of the whole discretized system. The eigenvectors of the undamped, autonomous system appear in complex conjugate pairs, i.e., $\mathbf{x}_n = \mathbf{y}_n + \mathrm{i}\mathbf{z}_n$, and $\bar{\mathbf{x}}_n = \mathbf{y}_n - \mathrm{i}\mathbf{z}_n$, where $\mathbf{y}_n$ and $\mathbf{z}_n$ are the real and imaginary parts of the eigenvector $\mathbf{x}_n$, respectively.

In order to save computation time, a modal truncation method is utilized here. Introduce a linear transformation $\mathbf{a} = \mathbf{U}\boldsymbol{\zeta}$, where $\mathbf{U}$ is the modal matrix formed by the real and imaginary parts of the first J normalized eigenvectors of the system, and $\boldsymbol{\zeta}$ is a generalized coordinate vector. Substituting this transformation into Eq. (3), premultiplying the transpose of $\mathbf{U}$ and using the orthogonality of eigenvectors yield the following partially uncoupled equations [21],

$$\dot{\zeta} + \boldsymbol{\Lambda}\boldsymbol{\zeta} = -\alpha\hat{\mathbf{C}}\boldsymbol{\zeta} + \frac{P_1(t)}{P_0}\hat{\mathbf{Q}}\boldsymbol{\zeta}, \tag{4}$$

where $\boldsymbol{\Lambda}$ is a block-diagonal matrix of the form

$$\boldsymbol{\Lambda} = \text{block} - \text{diag.}\begin{bmatrix} 0 & -\omega_n \\ \omega_n & 0 \end{bmatrix}, \quad \hat{\mathbf{C}} = \mathbf{U}^{\mathrm{T}}\begin{bmatrix} \mathbf{C} & 0 \\ 0 & 0 \end{bmatrix}\mathbf{U},$$

$$\hat{\mathbf{Q}} = P_0\mathbf{U}^{\mathrm{T}}\begin{bmatrix} 0 & \mathbf{K}_g \\ 0 & 0 \end{bmatrix}\mathbf{U}.$$

Note that $\hat{\mathbf{C}}$ is symmetric due to the property of the congruent transformation. The terms on the left-hand side of Eq. (4) are uncoupled in a block-wise sense, while those on the right-hand side of the equation are still coupled together. To match the form of the matrix $\boldsymbol{\Lambda}$, the matrices on the right-hand side of the equation are partitioned into J^2 blocks of 2×2 matrices. Therefore, Eq. (4) can be rewritten into the following form:

$$\begin{aligned}
\dot{\xi}_n - \omega_n\eta_n = & -\alpha\sum_{j=1}^{J}\left(c_{nj}^{11}\xi_j + c_{nj}^{12}\eta_j\right) \\
& + \frac{P_1(t)}{P_0}\sum_{j=1}^{J}\left(q_{nj}^{11}\xi_j + q_{nj}^{12}\eta_j\right), \\
\dot{\eta}_n + \omega_n\xi_n = & -\alpha\sum_{j=1}^{J}\left(c_{nj}^{21}\xi_j + c_{nj}^{22}\eta_j\right) \\
& + \frac{P_1(t)}{P_0}\sum_{j=1}^{J}\left(q_{nj}^{21}\xi_j + q_{nj}^{22}\eta_j\right) \\
& n = 1, 2, \ldots, J,
\end{aligned} \tag{5}$$

where ξ_n and η_n are the $(2n-1)$th and $2n$th entries of $\boldsymbol{\zeta}$; c_{nj}^{im} and q_{nj}^{im} are the i–mth entries of the n–jth blocks of $\hat{C}$ and $\hat{Q}$, respectively.

3. Stochastic averaging method

Usually the solutions of Eq. (5) are assumed as

$$\xi_n = a_n \cos\,\Phi_n, \quad \eta_n = -a_n \sin\,\Phi_n, \quad n = 1, 2, \ldots, J, \tag{6}$$

where $\Phi_n = \omega_n t + \phi_n$, in which a_n and ϕ_n are the amplitudes and phase angles of the system responses, respectively. If the damping factor α and the random excitation $P_1(t)$ are small in some sense such that α is of order ε, and $P_1(t)/P_0$ is of order $\varepsilon^{1/2}$, where ε is a small parameter, the stochastic averaging procedure can be

applied to obtain an Ito equation for each a_n [20,22]. This procedure is due originally to Stratonovich [23], and it may be considered as an extension of the well-known averaging method of Bogoliubov and Mitropolski to stochastic differential equations. It makes approximation of a physical process by a Markov process and converts a physical equation of the form

$$\frac{\mathrm{d}}{\mathrm{d}t}X_j(t) = \varepsilon f_j(\mathbf{X}, t) + \varepsilon^{1/2} g_{jr}(\mathbf{X}, t)\xi_r(t)$$

into an Ito equation. In the above equation, f_j and g_{jk} are deterministic functionals, and $\xi_r(t)$ are random excitations with zero means. By Ito's differential rule and taking the ensemble average yield a set of linear simultaneous equations for the mean-square responses $E[a_n^2]$, from which the mean-square stability of the system can be determined. However, the equations for the ensemble average of a_n ($E[a_n]$) are not linear such that the first-moment stability of the system cannot be obtained [20].

Usually, the stability of the mean and mean square of the response amplitudes is of main concern to structural engineers [24]. The mean square of the response amplitude is connected with the energy of the system. The former is governed by the first-moment equations, and the latter is governed by the second-moment equations of the system. In order to obtain the first-moment stability condition of the system, the solutions of Eq. (5) are assumed alternatively as

$$\xi_n = z_n \mathrm{e}^{\mathrm{i}\omega_n t} + \bar{z}_n \mathrm{e}^{-\mathrm{i}\omega_n t},\ \eta_n = \mathrm{i}(z_n \mathrm{e}^{\mathrm{i}\omega_n t} - \bar{z}_n \mathrm{e}^{-\mathrm{i}\omega_n t}), \quad n = 1, 2, \ldots, J, \tag{7}$$

where z_n and $\bar{z}_n$ are the complex conjugate responses of the system. Substituting Eq. (7) into Eq. (5), one can solve for z_n,

$$\dot{z}_n = \alpha f_n(\mathbf{z}, \bar{\mathbf{z}}; t) + \frac{P_1(t)}{P_0} g_n(\mathbf{z}, \bar{\mathbf{z}}; t), \quad n = 1, 2, \ldots, J, \tag{8}$$

where

$$\begin{aligned} f_n = & -\tfrac{1}{2}\sum_{r=1}^{J}[(c_{nr}^{11} + \mathrm{i}c_{nr}^{12} - \mathrm{i}c_{nr}^{21} + c_{nr}^{22}) z_r \mathrm{e}^{\mathrm{i}(\omega_r - \omega_n)t} \\ & + (c_{nr}^{11} - \mathrm{i}c_{nr}^{12} - \mathrm{i}c_{nr}^{21} - c_{nr}^{22}) \bar{z}_r \mathrm{e}^{-\mathrm{i}(\omega_r + \omega_n)t}], \\ g_n = & \tfrac{1}{2}\sum_{r=1}^{J}[(q_{nr}^{11} + \mathrm{i}q_{nr}^{12} - \mathrm{i}q_{nr}^{21} + q_{nr}^{22}) z_r \mathrm{e}^{\mathrm{i}(\omega_r - \omega_n)t} \\ & + (q_{nr}^{11} - \mathrm{i}q_{nr}^{12} - \mathrm{i}q_{nr}^{21} - q_{nr}^{22}) \bar{z}_r \mathrm{e}^{-\mathrm{i}(\omega_r + \omega_n)t}]. \end{aligned}$$

Assume that the damping factor α and the random excitation $P_1(t)$ are small in some sense such that α is of order ε, and $P_1(t)/P_0$ is of order $\varepsilon^{1/2}$. Hence, the stochastic averaging procedure can be applied to Eq. (8), and $\mathbf{z}$ can be uniformly approximated in the weak sense by a Markov vector [22], i.e.,

$$\mathrm{d}z_n = m_n \,\mathrm{d}t + \sum_{r=1}^{2J} \sigma_{nr} \,\mathrm{d}B_r, \quad n = 1, 2, \ldots, J, \tag{9}$$

where B_r are mutually independent unit Wiener processes; m_n are drift coefficients, and σ_{nr} are the n–rth element of the diffusion matrix $\boldsymbol{\sigma}$ with

$$\begin{aligned} m_n = & \langle \alpha f_n(\mathbf{z}, \bar{\mathbf{z}}; t) + \int_{-\infty}^{0} \{g_j(\mathbf{z}, \bar{\mathbf{z}}; t+\tau) \frac{\partial}{\partial z_j} g_n(\mathbf{z}, \bar{\mathbf{z}}; t) \\ & + \bar{g}_j(\mathbf{z}, \bar{\mathbf{z}}; t+\tau) \frac{\partial}{\partial \bar{z}_j} g_n(\mathbf{z}, \bar{\mathbf{z}}; t)\} R(\tau)\,\mathrm{d}\tau \rangle_t, \\ & n = 1, 2, \ldots, J, \end{aligned}$$

$$\left[\boldsymbol{\sigma}\sigma^{\mathrm{T}}\right]_{jk} = \left\langle \int_{-\infty}^{\infty} g_j(\mathbf{z},\bar{\mathbf{z}};t) g_k(\mathbf{z},\bar{\mathbf{z}};t+\tau) R(\tau)\,\mathrm{d}\tau \right\rangle_t$$

$$\left[\boldsymbol{\sigma}\sigma^{\mathrm{T}}\right]_{j(k+J)} = \left\langle \int_{-\infty}^{\infty} g_j(\mathbf{z},\bar{\mathbf{z}};t) \bar{g}_k(\mathbf{z},\bar{\mathbf{z}};t+\tau) R(\tau)\,\mathrm{d}\tau \right\rangle_t$$

$$j,k = 1,2,\ldots,J,$$

where $[\boldsymbol{\sigma}\sigma^{\mathrm{T}}]_{jk}$ is the j–kth entry of the product of the matrix $\boldsymbol{\sigma}$ and its transpose; $R(t)$ is the autocorrelation function of $P_1(t)/P_0$, and $\langle[\bullet]\rangle_t$ denotes a time-averaging operation with respect to t,

$$\langle[\bullet]\rangle_t = \lim_{T\to\infty} \frac{1}{2T} \int_{-T}^{T} [\bullet]\,\mathrm{d}t.$$

Going through the integrations, these coefficients can be obtained, and expressions of these coefficients are given in Appendix A.

Taking the ensemble average of Eq. (9) yields the first-moment equation for the mean response of the system,

$$\begin{aligned}\frac{\mathrm{d}}{\mathrm{d}t}E[z_n] = \Bigg\{ & -\frac{1}{2}\alpha\left(c_{nn}^{11}+c_{nn}^{22}\right) \\ & + \frac{1}{8}\sum_{r=1}^{J}[(q_{rn}^{11}+\mathrm{i}q_{rn}^{12}-\mathrm{i}q_{rn}^{21}+q_{rn}^{22})(q_{nr}^{11}+\mathrm{i}q_{nr}^{12} \\ & - \mathrm{i}q_{nr}^{21}+q_{nr}^{22})(S(\omega_n-\omega_r)-\mathrm{i}\psi(\omega_n-\omega_r)) \\ & + (q_{rn}^{11}+\mathrm{i}q_{rn}^{12}+\mathrm{i}q_{rn}^{21} \\ & - q_{rn}^{22})(q_{nr}^{11}-\mathrm{i}q_{nr}^{12}-\mathrm{i}q_{nr}^{21}-q_{nr}^{22})(S(\omega_n+\omega_r) \\ & -\mathrm{i}\psi(\omega_n+\omega_r))]\Bigg\}E[z_n], \\ & n = 1,2,\ldots,J, \end{aligned} \tag{10}$$

where $S(\omega)$ and $\psi(\omega)$ are the real and imaginary parts of the spectral density of $P_1(t)/P_0$, i.e., $S(\omega) = 2\int_0^\infty R(t)\cos\,\omega t\,\mathrm{d}t$, and $\psi(\omega) = 2\int_0^\infty R(t)\sin\,\omega t\,\mathrm{d}t$.
Note that in Eq. (10), the advantage of the symmetry property of the damping matrix is taken.

The first-moment equations are linear, uncoupled first-order ordinary equations. If the real part of the coefficient of the term on the right-hand side of each equation is negative, every mean response of the system is bounded, and vice versa. Consequently, the first-moment stability boundary of the system corresponds to the one that first makes a real part of the coefficient of the term on the right-hand side of an equation equal to 0.

The stability conditions become more restrictive with higher order of moments. Often the stability criterion of the first-order moment is a rather weak criterion, but it is found occasionally that the general size and location of the first moment stability region is more superior than the second-moment stability region [24]. Hence, the stability criterion of the second-moment is also adopted simultaneously to obtain more reliable results. By Ito's differential rule [22], the Ito differential equation for $z_n\bar{z}_n$ can be derived as

$$\begin{aligned}\mathrm{d}(z_n\bar{z}_n) = \{ & -\alpha\left(c_{nn}^{11}+c_{nn}^{22}\right) \\ & + \tfrac{1}{8}\sum_{r=1}^{J}\left[\left(q_{rn}^{11}-\mathrm{i}q_{rn}^{12}-\mathrm{i}q_{rn}^{21}+q_{rn}^{22}\right)\left(q_{rn}^{11}+\mathrm{i}q_{rn}^{12}\right.\right. \\ & - \mathrm{i}q_{nr}^{21}+q_{nr}^{22})(S(\omega_n-\omega_r)+\mathrm{i}\psi(\omega_n-\omega_r)) \\ & + (q_{rn}^{11}+\mathrm{i}q_{rn}^{12}+\mathrm{i}q_{rn}^{21} \\ & - q_{rn}^{22})(q_{nr}^{11}-\mathrm{i}q_{nr}^{12}-\mathrm{i}q_{nr}^{21}-q_{nr}^{22})z_n(S(\omega_n+\omega_r) \\ & + \mathrm{i}\psi(\omega_n+\omega_r)) \\ & + (q_{rn}^{11}+\mathrm{i}q_{rn}^{12}+\mathrm{i}q_{rn}^{21}+q_{rn}^{22})(q_{nr}^{11}-\mathrm{i}q_{nr}^{12}+\mathrm{i}q_{nr}^{21}+q_{nr}^{22})(S(\omega_n-\omega_r) \end{aligned}$$

$$
\begin{aligned}
&- \mathrm{i}\psi(\omega_n - \omega_r)) + (q_{rn}^{11} - \mathrm{i}q_{rn}^{12} - \mathrm{i}q_{rn}^{21} - q_{rn}^{22}) \\
&\times (q_{nr}^{11} + \mathrm{i}q_{nr}^{12} + \mathrm{i}q_{nr}^{21} - q_{nr}^{22})(S(\omega_n + \omega_r) - \mathrm{i}\psi(\omega_n + \omega_r))]\}z_n\bar{z}_n\,dt \\
&+ \tfrac{1}{8}\sum_{r=1}^{J}[(q_{nn}^{11} + \mathrm{i}q_{nn}^{12} - \mathrm{i}q_{nn}^{21} + q_{nn}^{22})(q_{nn}^{11} - \mathrm{i}q_{nn}^{12} + \mathrm{i}q_{nn}^{21} + q_{nn}^{22})S(0) \\
&+ (q_{nn}^{11} - \mathrm{i}q_{nn}^{12} - \mathrm{i}q_{nn}^{21} - q_{nn}^{22})(q_{nn}^{11} + \mathrm{i}q_{nn}^{12} + \mathrm{i}q_{nn}^{21} - q_{nn}^{22})S(2\omega_r)]z_r\bar{z}_r\,\mathrm{d}t \\
&+ \sum_{r=1}^{2J}(\sigma_{nr}\bar{z}_n\,\mathrm{d}B_r + \sigma_{(n+J)r}z_n\,\mathrm{d}B_r), \\
n &= 1, 2, \ldots, J. \qquad (11)
\end{aligned}
$$

Taking the ensemble average of Eq. (11) yields the second-moment equation for the mean-square response of the system. It is evident that the resulting equation will be the same as Eq. (11) with the stochastic terms being absent and the response variables $z_n\bar{z}_n$ replaced by their expectations, and the second-moment equation can be written as

$$\frac{\mathrm{d}}{\mathrm{d}t}\mathbf{Z} = \mathbf{B}\mathbf{Z}, \qquad (12)$$

where $\mathbf{Z} = \{E[z_1\bar{z}_1], E[z_2\bar{z}_2], ..., E[z_J\bar{z}_J]\}^{\mathrm{T}}$, and $\mathbf{B}$ is a constant coefficient matrix. The second-moment stability of the system is assured if the mean-square response of the system $\mathbf{Z}$ is bounded, which demands that the real parts of all eigenvalues of $\mathbf{B}$ be negative. Consequently, the second-moment stability criterion corresponds to the one that first renders the real part of an eigenvalue of $\mathbf{B}$ being 0.

4. Numerical results and discussions

As an application of the general solution, the random process $P_1(t)/P_0$ used to produce numerical results in this section is assumed as a Gaussian white noise with a spectral density S for simplicity. Therefore, $S(0) = S(2\omega_n) = S(\omega_j \pm \omega_k) = S$, and $\psi(2\omega_n) = \Psi(\omega_j \pm \omega_k) = 0$. However, numerical results for other random processes can also be generated easily. Moreover, unless otherwise mentioned, the bearing is assumed to be isotropic with $k_{YZ} = k_{ZY} = c_{YZ} = c_{ZY} = 0$, $k_{YY} = k_{ZZ}$ and $c_{YY} = c_{ZZ}$. In addition, all numerical results in this work are presented in non-dimensional forms: $\hat{X}_0 = X_0/L$, $\hat{M} = M/\rho AL$, $\hat{P}_0 = P_0L^2/EI$, $\hat{K} = k_{ZZ}L^3/EI$, $\alpha = c_{ZZ}/2\rho AL\omega_0$ and $\hat{\Omega} = \sqrt{\rho AL^4/EI}\Omega$, where E and ρ are Young's modulus and the mass density of the shaft, respectively; I and A are the second moment of area and the area of the shaft, respectively; ω_0 is the fundamental natural frequency of the corresponding non-rotating Timoshenko beam.

Before conducting the stability analysis, the free vibration of a spinning rotor-bearing system subjected to a pair of static axial forces at both ends is carried out first. Fig. 2 shows the whirl speeds of a rotor-bearing system subjected to a pair of static axial forces at the ends. The frequencies of the rotor-bearing system are calculated with eight uniform elements. In this figure, each mode of the rotor-bearing system splits into a backward mode and a forward mode due to the gyroscopic effect. As the rotating speed increases, the frequency curves of the backward modes go downwards, while those of the forward modes go upwards. It is observed that the whirl speeds of the first forward and backward modes with a whirl ratio 1 are very close and around 6.0.

Although the first-moment stability boundary of the system can be obtained from Eq. (10) by the above analysis, it is found in the course of numerical calculation that for reasonable values of the spectral density of the random axial excitation, the mean response of the rotor-bearing system is always stable, which explains the reason why the first-moment stability of the system cannot be derived if the solutions of Eq. (5) are assumed as the forms shown in Eq. (6). Therefore, from now on, only the second-moment stability of the rotor-bearing system is studied.

The convergence study of the modal truncation method is undertaken first, and the effect of the number of modes used in the modal truncation method on the second-moment stability boundary of a rotor-bearing system subjected to a pair of random axial forces at the ends is illustrated in Fig. 3. Fig. 3(a) presents the

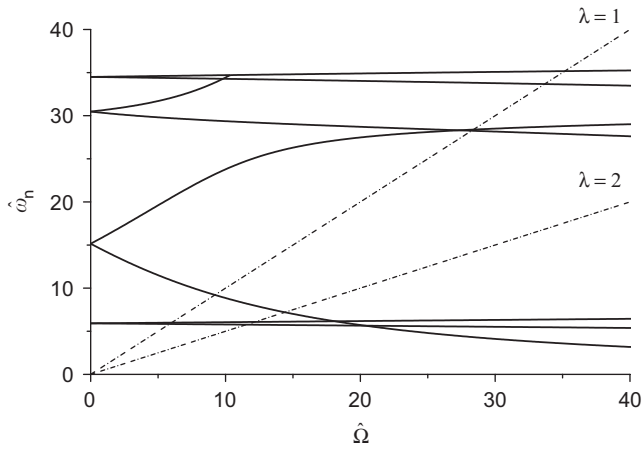

Fig. 2. The whirl speeds of a rotor-bearing system subjected to static axial forces at both ends. $\hat{M} = 0.5$, $\hat{X}_0 = 0.5$, $\sqrt{I/AL^2} = 0.1$, $\hat{K} = 700$, $\hat{P}_0 = 1.5$.

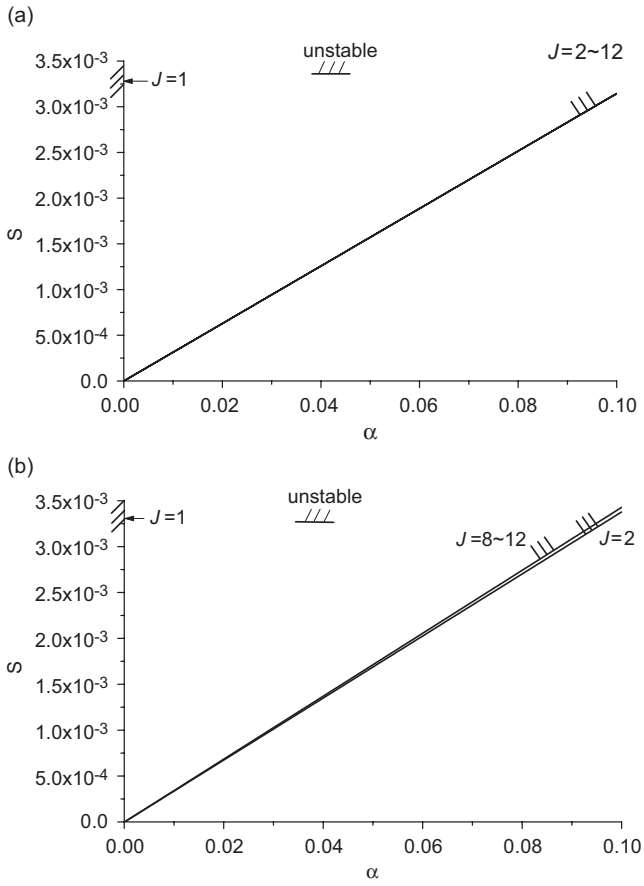

Fig. 3. Convergence studies of the second-moment stability boundary of a rotor-bearing system subjected to a pair of random axial forces at the ends. (a) $\hat{X}_0 = 0.5$; (b) $\hat{X}_0 = 0.125$. $\hat{M} = 0.5$, $\sqrt{I/AL^2} = 0.1$, $\hat{K} = 700$, $\hat{P}_0 = 1.5$, $\hat{\Omega} = 1.0$.

second-moment stability boundary of a rotor-bearing system with disk position $\hat{X}_0 = 0.5$; Fig. 3(b) presents the stability boundary with disk position $\hat{X}_0 = 0.125$. The second-moment stability boundary on the $S-\alpha$ plane is a straight line originated from the origin because all the entries of the coefficient matrix **B** in Eq. (12)

are functions of the ratio S/α for a Gaussian white noise excitation $P_1(t)/P_0$. The unstable region lies above the stability boundary. It means that the system needs a heavier bearing damping and a weaker random axial excitation to become stable. Therefore, the effect of the viscous damping of the bearing is stabilizing, while the effect of the random part of the axial force is destabilizing. As the number of modes J increases, the stability boundary rotates clockwise about the origin, leaving a larger unstable region. Consequently, the stability condition predicted is generally not conservative enough before the convergence is reached. Fig. 3(a) shows that if the disk is placed at the midpoint of the shaft, due to the symmetry, only the first two modes used in the modal truncation method are enough to get a convergent stability boundary. However, if the disk is placed at $\hat{X}_0 = 0.125$, it needs to use the first eight modes to obtain a convergent stability boundary, according to Fig. 3(b).

Fig. 4 depicts the second-moment stability boundary of a rotor-bearing system subjected to a pair of random axial forces at the ends for different values of β, where $\beta = cL/c_{ZZ}$ is the ratio of the non-rotating viscous damping of the shaft to the bearing damping. The lowest curve represents the stability boundary of the rotor-bearing system with an undamped shaft. It is observed that increasing the non-rotating viscous damping of the shaft will raise the stability boundary and stabilize the rotor-bearing system. However, the stabilizing effect of the non-rotating viscous damping of the shaft is less effective than that of the bearing damping. Consequently, only the effect of the bearing damping is considered hereafter. Moreover, the stability boundaries are nearly a straight line sprouted from the origin for small $\hat{\Omega}$ and become flat for a further increase in $\hat{\Omega}$. It means that although an increase in the rotating speed will lower all frequencies of the backward modes, the effect of the rotating speed is favorable to the second-moment stability of the rotor-bearing system for low rotating speeds in the subcritical range. However, this effect will become destabilizing for very high rotating speeds in the supercritical range.

Fig. 5 shows the effect of the average axial force on the second-moment stability boundary of the rotor-bearing system. All the stability boundaries drop down drastically and approach the abscissa as the average axial compressive force increases. The stability boundary will touch the abscissa at $\hat{P}_0 = 7.68$, which is the critical buckling load of the spinning rotor-bearing system, beyond which the system is unstable (buckled) even though the random part of the axial force is absent. Before the rotor-bearing system is buckled, it can be dynamically unstable due to the random part of the axial force. Hence, the effect of the average axial compressive force is unfavorable to the second-moment stability of the system, and this is related to the fact that an increase in the static axial compressive load will decrease all frequencies of the rotor-bearing system.

The effect of the stiffness of the isotropic bearing on the second-moment stability boundary of the rotor-bearing system is presented in Fig. 6. The stability boundaries fall down very quickly and draw near to the

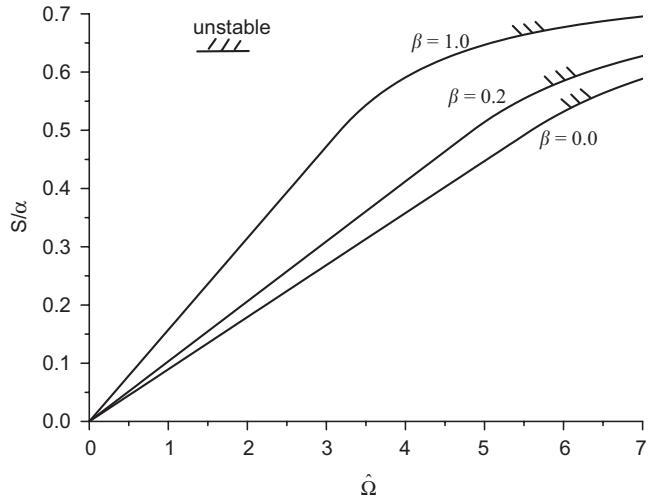

Fig. 4. The effect of the non-rotating viscous damping of the shaft on the second-moment stability boundary of a rotor-bearing system subjected to a pair of random axial forces at the ends. $\hat{M} = 0.5$, $\hat{X}_0 = 0.5$, $\sqrt{I/AL^2} = 0.1$, $\hat{K} = 700$, $\hat{P}_0 = 1.5$.

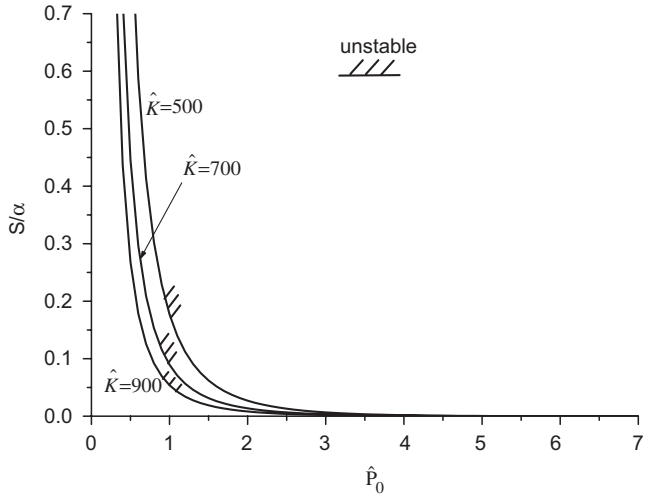

Fig. 5. The effect of the average axial force on the second-moment stability boundary of a rotor system supported by a pair of ball bearings at the ends. $\hat{M} = 0.5$, $\hat{X}_0 = 0.5$, $\sqrt{I/AL^2} = 0.1$, $\hat{K} = 700$, $\hat{\Omega} = 1.0$.

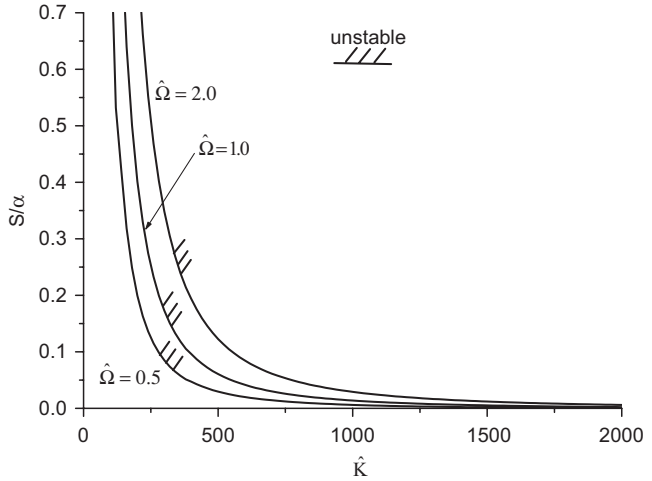

Fig. 6. The effect of the bearing stiffness on the second-moment stability boundary of a rotor-bearing system subjected to a pair of random axial forces at the ends. $\hat{M} = 0.5$, $\hat{X}_0 = 0.5$, $\sqrt{I/AL^2} = 0.1$, $\hat{P}_0 = 1.5$, $\hat{\Omega} = 1.0$.

abscissa as the bearing stiffness increases. Therefore, the effect of the bearing stiffness is undesirable to the second-moment stability of the system although an increase in the bearing stiffness will raise all frequencies of the rotor-bearing system. Fig. 7 show the second-moment stability boundary of a rotor-bearing system with either isotropic or orthotropic bearings at the ends. In this figure, the stiffness and damping coefficients of the orthotropic bearings are given as

$$\begin{bmatrix} c_{YY} & c_{YZ} \\ c_{ZY} & c_{ZZ} \end{bmatrix} = c_{ZZ} \begin{bmatrix} 1.0 & -0.25 \\ -0.25 & 1.0 \end{bmatrix},$$

$$\begin{bmatrix} k_{YY} & k_{YZ} \\ k_{ZY} & k_{ZZ} \end{bmatrix} = k_{ZZ} \begin{bmatrix} 1.0 & -0.25 \\ -0.25 & 1.0 \end{bmatrix}.$$

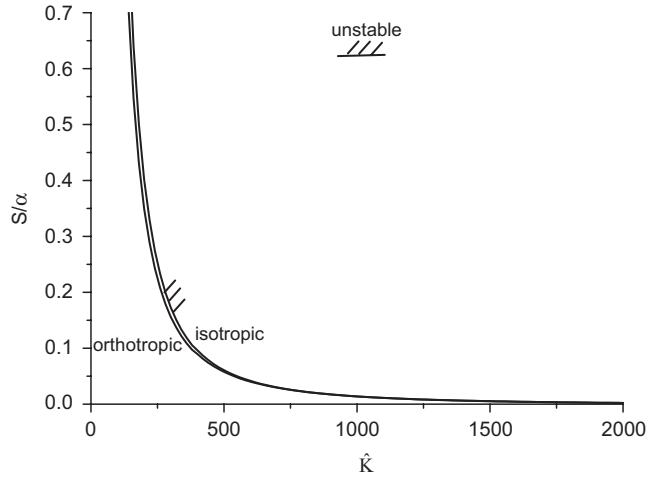

Fig. 7. The second-moment stability boundary of a rotor system supported by either isotropic or orthotropic bearings at the ends. $\hat{M} = 0.5$, $\hat{X}_0 = 0.5$, $\sqrt{I/AL^2} = 0.1$, $\hat{P}_0 = 1.5$, $\hat{\Omega} = 1.0$.

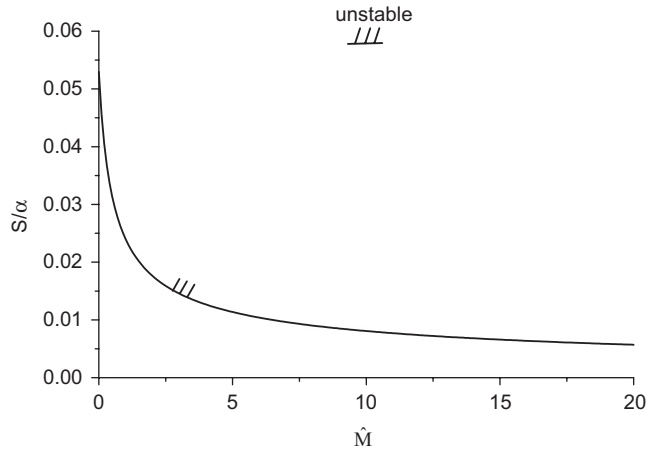

Fig. 8. The effect of the disk mass on the second-moment stability boundary of a rotor-bearing system subjected to a pair of random axial forces at the ends. $\hat{X}_0 = 0.5$, $\sqrt{I/AL^2} = 0.1$, $\hat{K} = 700$, $\hat{P}_0 = 1.5$, $\hat{\Omega} = 1.0$.

This symmetric bearing is equivalent to an orthotropic bearing with principal axes oriented 45° and 135° relative to the Y-axis. It is observed that both stability boundaries are very close, and the rotor-bearing system with isotropic bearings at the ends is more stable than the system with orthotropic bearings.

Fig. 8 illustrates the effect of the disk mass on the second-moment stability boundary of the rotor-bearing system. The stability boundary goes down gradually as the disk mass increases. Consequently, the effect of the disk mass is destabilizing in the sense of the second-moment stability, and this can be connected with the fact that an increase in the disk mass will decrease all frequencies of the rotor-bearing system. Fig. 9 depicts the effect of the disk position on the second-moment stability boundary of the rotor-bearing system. The stability boundary is symmetric with respect to the midpoint of the shaft because of the configuration symmetry. The rotor-bearing system is most unstable if the disk is placed at the midpoint of the shaft, and, in this case, is most stable if the disk is placed at about the quarter-point of the shaft. This may be attributed to the reason that the gyroscopic moment of the disk causes an increase in the critical speeds of the rotor-bearing system if the thin disk is not located at the midpoint of the shaft [12].

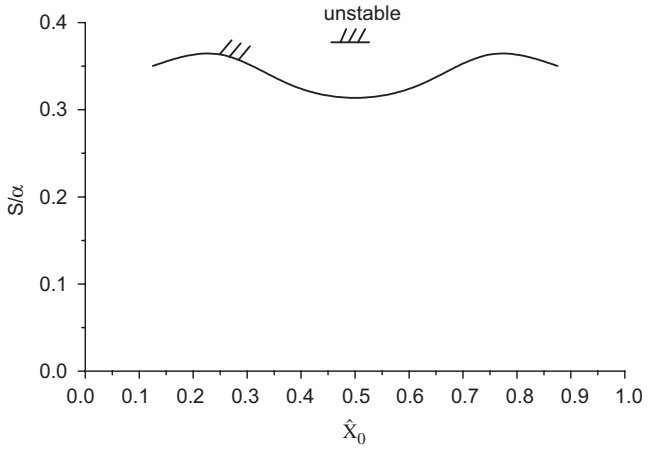

Fig. 9. The effect of the disk position on the second-moment stability boundary of a rotor-bearing system subjected to a pair of random axial forces at the ends. $\hat{M} = 0.5$, $\sqrt{I/AL^2} = 0.1$, $\hat{K} = 700$, $\hat{P}_0 = 1.5$, $\hat{\Omega} = 1.0$.

5. Conclusions

The dynamic stability of a spinning disk–shaft system supported by a pair of ball bearings and subjected to a pair of random axial forces at both ends is analyzed in this work. The axial forces are assumed as the sum of a static force and a random process with a zero mean. Due to the random qpart of the axial forces, the rotor-bearing system may experience parametric random instability under certain situations. By suitable assumption of the form of the system response, the first- and second-moment stability criteria of the system can be determined. Numerical results are given for a Gaussian white noise excitation. In the course of numerical calculation, it is found that for reasonable values of the spectral density of the random axial excitation, the first-moment response of the rotor-bearing system is always stable. Therefore, only second-moment stability results are presented in this work.

The effects of various system parameters on the second-moment stability of the rotor-bearing system were investigated, and the following conclusions can be drawn:

(1) The second-moment stability boundary of the rotor-bearing system on the $S-\alpha$ plane is a straight line originated from the origin, and the stability boundary depends only on the ratio S/α if the random part of the axial force is a Gaussian white noise.
(2) Convergence of the number of modes used in the modal truncation method to produce the second-moment stability results depends on the disk position. If the disk is placed at the midpoint of the shaft, only the first two modes are enough to get a convergent stability boundary. However, if the disk is placed at other position, it needs to use more modes to obtain a convergent stability boundary. Before the convergence is reached, the stability condition predicted is generally not conservative enough. Moreover, the rotor-bearing system is most unstable if the disk is placed at the midpoint of the shaft.
(3) The effects of the average axial compressive force and disk mass, which will lower all frequencies of the system, tend to destabilize the second-moment stability of the rotor-bearing system.
(4) The effect of the rotating speed is favorable to the second-moment stability of the rotor-bearing system for low rotating speeds and becomes destabilizing for very high rotating speeds.
(5) The effects of the non-rotating viscous damping of the shaft and the bearing damping are stabilizing, but the effect of the bearing stiffness is undesirable to the second-moment stability of the system. The rotor-bearing system with isotropic bearings at both ends is a little more stable than the system with orthotropic bearings at both ends.

Appendix A

$$
\begin{aligned}
m_n = \{ & -\tfrac{1}{2}\alpha(c_{nn}^{11} + c_{nn}^{22})z_n \\
& + \tfrac{1}{8}\sum_{r=1}^{J}[(q_{rn}^{11} + \mathrm{i}q_{rn}^{12} - \mathrm{i}q_{rn}^{21} + q_{rn}^{22}) \\
& \times (q_{nr}^{11} + \mathrm{i}q_{nr}^{12} - \mathrm{i}q_{nr}^{21} + q_{nr}^{22})z_n(S(\omega_n - \omega_r) - \mathrm{i}\psi(\omega_n - \omega_r)) \\
& + (q_{rn}^{11} + \mathrm{i}q_{rn}^{12} + iq_{rn}^{21} - q_{rn}^{22})(q_{nr}^{11} \\
& - \mathrm{i}q_{nr}^{12} - \mathrm{i}q_{nr}^{21} - q_{nr}^{22})z_n(S(\omega_n + \omega_r) - \mathrm{i}\psi(\omega_n + \omega_r))]\} \\
& n = 1, 2, \ldots, J,
\end{aligned}
$$

$$
\begin{aligned}
[\boldsymbol{\sigma}\sigma^{\mathrm{T}}]_{jk} = \tfrac{1}{4}[& (q_{jj}^{11} + \mathrm{i}q_{jj}^{12} - \mathrm{i}q_{jj}^{21} + q_{jj}^{22}) \\
& (q_{kk}^{11} + \mathrm{i}q_{kk}^{12} - \mathrm{i}q_{kk}^{21} + q_{kk}^{22})z_j z_k S(0) \\
& + (q_{jk}^{11} + \mathrm{i}q_{jk}^{12} - \mathrm{i}q_{jk}^{21} + q_{jk}^{22}) \\
& (q_{jk}^{11} + \mathrm{i}q_{jk}^{12} - \mathrm{i}q_{jk}^{21} + q_{jk}^{22})z_j z_k S(\omega_j - \omega_k)],
\end{aligned}
$$

$$
\begin{aligned}
[\boldsymbol{\sigma}\sigma^{\mathrm{T}}]_{j(k+J)} = \tfrac{1}{4}[& (q_{jj}^{11} - \mathrm{i}q_{jj}^{12} + \mathrm{i}q_{jj}^{21} + q_{jj}^{22}) \\
& \times (q_{kk}^{11} + \mathrm{i}q_{kk}^{12} - \mathrm{i}q_{kk}^{21} + q_{kk}^{22})\bar{z}_j z_k S(0) \\
& + (q_{jk}^{11} + \mathrm{i}q_{jk}^{12} + \mathrm{i}q_{jk}^{21} - q_{jk}^{22}) \\
& \times (q_{kj}^{11} - \mathrm{i}q_{kj}^{12} - \mathrm{i}q_{kj}^{21} - q_{kj}^{22})\bar{z}_j z_k S(\omega_j + \omega_k)] \\
& j, k = 1, 2, \ldots, J.
\end{aligned}
$$

References

[1] S.H. Crandall, P.J. Brosens, On the stability of rotation of a rotor with rotationally unsymmetric inertia and stiffness properties, *Journal of Applied Mechanics* 83 (1961) 567–570.

[2] D.E. Bently, The re-excitation of balance resonance regions by internal friction, *ASME Paper No.* 72-PET-49 (1972).

[3] A.D. Dimaragonas, S.A. Paipetis, *Analytical Methods in Rotor Dynamics*, Applied Science Publishers, London, 1983.

[4] J.M. Vance, *Rotordynamics of Turbomachinery*, Wiley, New York, 1988.

[5] M. Lalanne, G. Ferraris, *Rotordynamics Prediction in Engineering*, Wiley, Chichester, 1990.

[6] D. Childs, *Turbomachinery Rotordynamics*, Wiley, New York, 1993.

[7] J.S. Rao, *Rotor Dynamics*, New Age International Publishers, New Delhi, 1996.

[8] A. Muszynska, *Rotordynamics*, Taylor & Francis Group, Boca Raton, 2005.

[9] H.D. Nelson, J.H. McVaugh, The dynamics of rotor-bearing systems using finite elements, *Journal of Engineering for Industry* 98 (1976) 593–600.

[10] H.D. Nelson, A finite rotating shaft element using Timoshenko beam theory, *Journal of Mechanical Design* 102 (1980) 793–803.

[11] H. Nevzat Ozguven, Z. Levent Ozkan, Whirl speeds and unbalance response of multibearing rotors using finite elements, *Journal of Vibration, Acoustics, Stress, and Reliability in Design* 106 (1984) 72–79.

[12] G. Genta, *Vibration of Structures and Machines*, Springer, New York, 1993.

[13] L.W. Chen, D.M. Ku, Dynamic stability analysis of a rotating shaft by the finite element method, *Journal of Sound and Vibration* 143 (1990) 143–151.

[14] L.W. Chen, W.K. Peng, Dynamic stability of rotating composite shafts under periodic axial compressive loads, *Journal of Sound and Vibration* 212 (1998) 215–230.

[15] C.-L. Liao, B.-W. Huang, Parametric instability of a spinning pretwisted beam under periodic axial force, *International Journal of Mechanical Science* 37 (1995) 423–439.

[16] J.K. Park, K.W. Kim, Stability analyses and experiments of spindle system using new type of slot-restricted gas journal bearings, *Tribology International* 37 (2004) 451–462.

[17] B.W. Huang, The crack effect on instability in a machine tool spindle with gas bearings, *Journal of Sound and Vibration* 286 (2005) 1001–1018.

[18] B.W. Huang, H.K. Kung, Variations of instability in a rotating spindle system with various bearings, *International Journal of Mechanical Science* 45 (2003) 57–72.

[19] N. Sri Navachchivaya, Mean-square stability of a rotating shaft under combined harmonic and stochastic excitations, *Journal of Sound and Vibration* 133 (1989) 323–336.
[20] T.H. Young, C.Y. Gau, Dynamic stability of spinning pretwisted beams subjected to axial random forces, *Journal of Sound and Vibration* 268 (2003) 149–165.
[21] L. Meirovitch, *Principles and Techniques of Vibrations*, Prentice-Hall, Inc., Englewood Cliffs, NJ, 1997.
[22] Y.K. Lin, G.Q. Cai, *Probabilistic Structural Dynamics*, McGraw-Hill, Inc., New York, 1995.
[23] R.L. Stratonovich, *Topics in the Theory of Random Noise*, Vol. 1, Gordon and Breach, New York, 1963.
[24] R.A. Ibrahim, *Parametric Random Vibration*, Wiley, New York, 1985.